Heliyon 10 (2024) e24562

Contents lists available at ScienceDirect

Heliyon

journal homepage: www.cell.com/heliyon

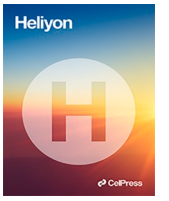

Research article

Pterostilbene attenuates heart failure by inhibiting myocardial ferroptosis through SIRT1/GSK-3β/GPX4 signaling pathway

Fan Zhang [a,d,e,1], Zhuanglin Zeng [c,1], Jiahui Zhang [a,d,e], Xuelian Li [a,d,e], Wenling Yang [a,d,e], Yumiao Wei [a,d,e,**], Xiaopeng Guo [b,*]

[a] *Department of Cardiology, Union Hospital, Tongji Medical College, Huazhong University of Science and Technology, Wuhan, 430022, China*
[b] *Department of Radiology, Union Hospital, Tongji Medical College, Huazhong University of Science and Technology, Wuhan, 430022, China*
[c] *Department of Emergency Medicine, Union Hospital, Tongji Medical College, Huazhong University of Science and Technology, Wuhan, 430022, China*
[d] *Hubei Key Laboratory of Biological Targeted Therapy, Union Hospital, Tongji Medical College, Huazhong University of Science and Technology, Wuhan, China*
[e] *Hubei Engineering Research Center for Immunological Diagnosis and Therapy of Cardiovascular Diseases, Union Hospital, Tongji Medical College, Huazhong University of Science and Technology, Wuhan, China*

ARTICLE INFO

Keywords:
Pterostilbene
Ferroptosis
Heart failure
Cardiac remodeling
SIRT1/GSK-3β/GPX4 signaling

ABSTRACT

Sustained myocardial injury due to hypertension and diabetes mellitus leads to production of endogenous reactive oxygen species (ROS) and insufficient myocardial antioxidant capacity, increasing the risk of cardiomyocyte ferroptosis. Ferroptosis is a nonapoptotic form of cell death driven by unrestricted lipid peroxidation. Dysfunction of the glutathione peroxidase 4 (GPX4) antioxidant system also plays an important role in ferroptosis. Cardiomyocyte ferroptosis ultimately leads to myocardial deterioration, such as inflammation, fibrosis, and cardiac remodeling, resulting in structural and functional changes. Pterostilbene (PTS), a demethylated derivative of resveratrol, exhibits strong anti-inflammatory and antioxidative activities. In this study, we used *in vitro* experiments to explore ferroptosis induced by angiotensin II (Ang II) of primary cardiac myocytes (CMs) and *in vivo* experiments to prepare a transverse aortic constriction (TAC)-induced cardiac dysfunction mouse model. PTS can significantly ameliorate Ang II-induced cardiomyocyte ferroptosis *in vitro* and reduce cardiac remodeling, while improving cardiac function in mice after TAC *in vivo*. Further mechanistic investigations revealed that PTS exerts its protective effect through the SIRT1/GSK-3β/GPX4 pathway. After siRNA-mediated knockdown of SIRT1 or GPX4 in CMs, the protective effects of PTS on cardiomyocytes were abolished. This study provides important theoretical support for the potential of PTS to attenuate pathological cardiac remodeling and heart failure and provides a preliminary exploration of the molecular pathways involved in its protective mechanism.

* Corresponding author.
** Corresponding author. Department of Cardiology, Union Hospital, Tongji Medical College, Huazhong University of Science and Technology, Wuhan 430022, China.
E-mail addresses: yumiao_wei@hust.edu.cn (Y. Wei), 2018xh0095@hust.edu.cn (X. Guo).
[1] Equal contributions to this work.

https://doi.org/10.1016/j.heliyon.2024.e24562
Received 1 September 2023; Received in revised form 15 December 2023; Accepted 10 January 2024
Available online 20 January 2024

1. Introduction

Cardiovascular disease is a major threat to human life and health. Heart failure (HF) is a global epidemic. There were an estimated 64.3 million prevalent cases of heart failure globally in 2017 [1]. Unfortunately, mortality from heart failure has always been high. As reported, heart failure–related hospitalizations increase the excess deaths by 10 %–30 % [2], and the median survival for heart failure was only 2.1 years [3]. Hypertension, aortic stenosis, and other conditions that cause long-term increases in ventricular afterload are common risk factors for heart failure [4]. More than a quarter of people worldwide are considered to have hypertension. It was reported that hypertension is associated with a 71 % increase in the risk of heart failure [5]. Up to a quarter of patients with severe aortic stenosis may eventually heart failure [6]. Chronic pressure overload leads to cardiac remodeling, culminating in decreased cardiac compliance and heart failure [7]. In addition to hypertension, diabetes is also an independent risk factor for HF, which increases the risk of heart failure by 2- to 4-fold. 8.5 % of adults $\geq$18 years had diabetes [8]. Diabetes causes myocardial ischemia through vasculopathy, and can also directly damage the function of the myocardium. Chronic heart failure (CHF) results from multiple cardiovascular diseases and is associated with poor prognosis [9]. Inflammatory damage and oxidative stress play crucial roles in this process. Myocardial injury increases the production of endogenous reactive oxygen species (ROS), which aggravate the deterioration of cardiac function [10]. Despite advances in HF treatment over the past few decades, its prevalence and hospitalization rates continue to increase. Therefore, it is important to elucidate the mechanisms of HF progression and explore new methods to improve cardiac function.

The term ferroptosis was originally defined in 2012 as an iron-dependent form of nonapoptotic cell death [11]. It is one of the most widespread forms of cell death. Compared with regulatory cell death, ferroptosis is not triggered by protease activation of the caspase family but driven by lipid peroxidation. The canonical axis of ferroptosis-controlling requires uptake of cystine, which is subsequently reduced to cysteine within the cell, promoting GSH biosynthesis and ultimately leads to increased intracellular content of the antioxidant glutathione peroxidase 4 (GPX4). GPX4 can mediate the reduction of any hydrogen peroxide phospholipids (PLOOHs). Ferroptosis is characterized by ROS production and lipid peroxidation. It is regulated by multiple metabolic pathways, such as mitochondrial viability, intracellular iron status and amino acid metabolism. Disturbances in iron metabolism are essential for ROS production and lipid peroxides activation [12]. The increased intracellular free Fe^{2+} produced through the Fenton reaction mediates the massive production of ROS and rapid amplification of PLOOHs on membranes, resulting in the inhibition of the antioxidant glutathione peroxidase 4 (GPX4) [13]. This process eventually leads to ferroptosis. The normal function of GPX4 is central to the control of ferroptosis, and GPX4 inhibition/instability can trigger cellular ferroptosis. GPX4 can reduce cholesterol and phospholipid hydroperoxide levels, thus interrupting the lipid peroxidation chain reactions [14,15]. Ferroptosis is associated with pathophysiological processes in various diseases, such as cancer, stroke, ischemia, and reperfusion injury. Ferroptosis has also been shown to influence the development of HF caused by various conditions such as cardiomyopathy and myocardial infarction [16]. Recent studies have shown that cardiomyocyte ferroptosis plays an important role in HF and cardiac remodeling [17,18]. In animal models of cardiac hypertrophy, infusion of Ang II and pressure overload cause HF. In a 1-year follow-up study of patients with chronic HF, malondialdehyde (MDA) was found to be an independent predictor of death [19]. This result supports the hypothesis that the inhibition of ferroptosis may be an effective treatment for chronic HF.

Sirtuins (SIRTs) are members of the NAD-dependent deacetylase enzyme family that regulate various cellular functions; among them, Sirtuin 1 (SIRT1) is the most extensively studied. Previous studies have shown that SIRT1 alleviates liver and acute kidney injury in mice by inhibiting ferroptosis [20,21]. The cardioprotective effects of SIRT1 have also been demonstrated [22,23]. Glycogen synthase kinase-3β (GSK-3β) is an evolutionarily conserved serine/threonine kinase that is involved in multiple signaling pathways and a variety of cellular metabolic processes. Its depletion reduces the unstable free iron pool in cells by disrupting the cellular iron metabolism, which can lead to embryonic death. Increasing evidence has proven that potential therapeutic applications targeting GSK-3β could be used to treat common diseases, such as cancer, inflammatory diseases, neurodegenerative diseases [24], and psychiatric disorders [25–28]. Z-disc GSK-3β levels are reduced in patients with HF [29]. The phosphorylation of GSK-3β (p-GSK-3β) induces myocardial injury by increasing the expression of caspase-3 and Bcl-2-associated X protein (Bax)/B cell lymphoma 2 protein (Bcl-2) in cardiomyocytes [30]. It also acts as a downstream molecule of SIRT1 to regulate ferroptosis [31].

Pterostilbene (PTS), also known as 3,5-dimethoxy-4′-hydroxystilbene, is a dimethylated analog of resveratrol. PTS is a constituent of the deciduous tree *Pterocarpus marsupium* and is most abundantly found in blueberries. PTS has anti-inflammatory, antioxidant, anticancer, and neuroprotective properties [32,33]. PTS induces autophagy and regulates Nrf2-mediated antioxidant pathways in melanocytes [34]. Furthermore, previous studies in HF confirmed that PTS could reduce oxidative stress and inflammation through the Nrf2/NF-κB signaling pathway [35]. PTS also modulates calcium-handling proteins to improve right ventricular function [36]. In a study on liver fibrosis and intestinal injury, PTS was confirmed to regulate SIRT1 [37,38]. At present, the effects and exact mechanisms of PTS on cardiomyocyte ferroptosis and HF remain unclear. Therefore, we investigated the role of PTS in transverse aortic constriction (TAC) and angiontensin II (Ang II)-induced HF models and explored the molecular pathways that may be involved.

2. Materials and methods

2.1. Animals

C57BL/6 male mice (8–10 weeks old) were acquired from Hua Fukang Experimental Animal Center (Beijing, China) and housed in the Center for Specific Pathogen-Free Animals, Tongji Medical College, Huazhong University of Science and Technology. Mice are kept in cages with free access to water and food. Dividing mice randomly into three groups (n = 10): sham, TAC, TAC + PTS (PTS, 50 mg/kg). All procedures were approved by the Experimental Animal Research Committee of Tongji Medical College.

2.2. Transverse aortic constriction (TAC)

10-week-old male C57BL/6J mice were selected for TAC surgery. They were anesthetized with 3 % sodium pentobarbital and fixed on the operating table. Then artificial ventilation was performed with a special mouse ventilator. An experimental needle was made with a 27G needle. Opening the chest cavity to expose the aortic arch, then the aortic arch between the artery and the left carotid artery was attached to the experimental needle by a 6-0 thread to ensure narrowing of arterial arches in experimental mice. The needle was then lightly removed, which would leave a 70 % of the constriction. Mice in the sham-operated group underwent a similar operation except for the contraction of the aortic arch. The mice continued to be fed for 8 weeks after surgery. Mice that underwent sham operation were classified as control group and those underwent arterial arches narrowing were classified as TAC group.

2.3. Echocardiography

After 8 weeks of treatment, echocardiography was performed in mice under sevoflurane anesthesia. Placing the mice in supine position on a heating pad and echocardiography was performed with the use of a mouse high-frequency imaging system (Vevo 3100). After that, collecting the parameters of cardiac function including left ventricular ejection fraction (EF%), left ventricular fractional shortening (FS%), left ventricular internal dimension at diastole (LVIDd), left ventricular internal dimensions at systole (LVIDs) and cardiac output per minute (CO).

2.4. Heart weighing

After the echocardiogram, the mice were immediately weighed. Taking heart tissue according to a uniform standard and weighing the heart. The heart weight ratio (heart weight/body weight, HW/BW) and the ratio of heart weight/tibia length (HW/TL) was calculated.

2.5. Histological analysis and immunofluorescence staining

The heart was first fixed with 4 % formaldehyde and then dehydrated, embedded in paraffin wax, and sectioned. Immersing heart paraffin sections in 3 % hydrogen peroxide solution and then retrieving the antigen. Cell membranes were permeabilized and sealed with 0.25 % TritonX-100 and fetal donkey serum respectively. Cardiac pathology was visualized by haematoxylin and eosin (H&E), Masson's trichrome, wheat germ agglutinin (WGA) staining (#L4895, Sigma, USA) and then cardiac fibrosis and hypertrophy were measured. GPX4 (#67763-1-lg, Proteintech, USA) fluorescence staining of myocardial tissue and cardiomyocytes was performed according to instructions. Image J-Pro Plus 6.0 software (Media Cybemetics, Bethesda, USA) was used to calculate the data.

2.6. Transmission electron microscope (TEM)

Dicing the mouse heart tissue into 2 mm thickness, then pre-fixing them in 3 % glutaraldehyde for 2 h. After washing by phosphate buffe, samples were then fixed in 1 % osmic acid fixative solution. Samples were washed again by phosphate buffer and dehydrated with acetone, then embedded in Epon/SPURR resin. The heart tissues were washed 3–5 times in distilled water after sectioning, then stained with 0.2 % lead citrate. Images were taken by an electron microscope.

2.7. Culture of primary cardiac myocytes (CMs) and H9C2 cells

CMs were isolated from 1 to 3 days-old C57BL/6 hearts. Mouse hearts were removed under aseptic conditions and washed in D-HANKS equilibrium solution. All hearts were cut and digested with pancreatic enzymes for 30 min, then the heart tissue was washed again. After that, the heart tissue was digested using 1 % type II collagenase (#17101-015, Gibco, USA) for 5 min, and the supernatant was taken into DMEM medium with 20 % fetal bovine serum (FBS). Repeat the procedure 6 times and collect the heart cells. The cells were inoculated into culture plates, and after 1 h the supernatant was taken and centrifuged. The collected cells were used to re-seed the plate to obtain cardiomyocytes of higher purity. Then the cells were subjected to treatment with or without 100 μg/ml PTS (#S3937, Selleck Chemicals, USA) and 100 nM Ang II (#A9525, Sigma-Aldrich, USA) for 48 h. H9C2 cells were cultured in DMEM medium with 10 % FBS. A 37 °C constant temperature incubator supplied with 5 % CO2 provides cells with a suitable living environment. The treatment of H9C2 cells was similar to that of CMs. Differently, CMs were used for staining experiments, and H9C2 cells were used for western blots. Cells in the control group were not stimulated by Ang II or treated with PTS. Cells in the Ang II group were stimulated by ANG but not treated with PTS, and cells in the ANG + PTS group were treated with both Ang II and PTS.

2.8. Small interference RNA (siRNA) transfection

Transfection was performed when the density of H9C2 cells reached 30–50 %. The complete DMEM medium was discarded and the cells were washed three times with PBS. The final concentration of siSIRT1 or siGPX4 was 50 nM at the time of transfection. siRNA was transfected with lipofectamine 3000 (#L3000-015, Invitrogen, USA) and steps were as follows. Diluting siRNA with 50 μl Opti-MEM firstly, then dissolving 5 μl lipofectamine 3000 in 245 μl Opti-MEM and leave it for 5 min at room temperature after mixed well. The transfection reagents and siRNA dilution were then mixed and left at room temperature for 20 min. Finally, the transfection complex

Table 1
The antibodies in Western blot.

Antibody	Source and reactivity	Dilution ratio	Manufacturer	Cat.No.
GPX4	Rabbit-Mouse, Rat, Human	1:1000	Abcam	ab219592
SIRT1	Mouse-Mouse, Rat, Human	1:1000	Abcam	ab110304
Ferritin	Rabbit -Human, Mouse, Rat	1:1000	ABclonal	A19544
GSK-3β	Rabbit -Human, Mouse, Rat, Monkey	1:1000	Cell Signaling Technology	12,456
Phospho- GSK-3β	Rabbit -Human, Mouse, Rat, Hamster	1:1000	Cell Signaling Technology	5558
GAPDH	Mouse-Human, Mouse, Rat, Yeast, Plant, Zebrafish	1:3000	Proteintech	60004-1-Ig
Goat-rabbit IgG	Goat-Rabbit	1:3000	Proteintech	SA00001-2
Goat-mouse IgG	Goat-Mouse	1:3000	Proteintech	SA00001-1

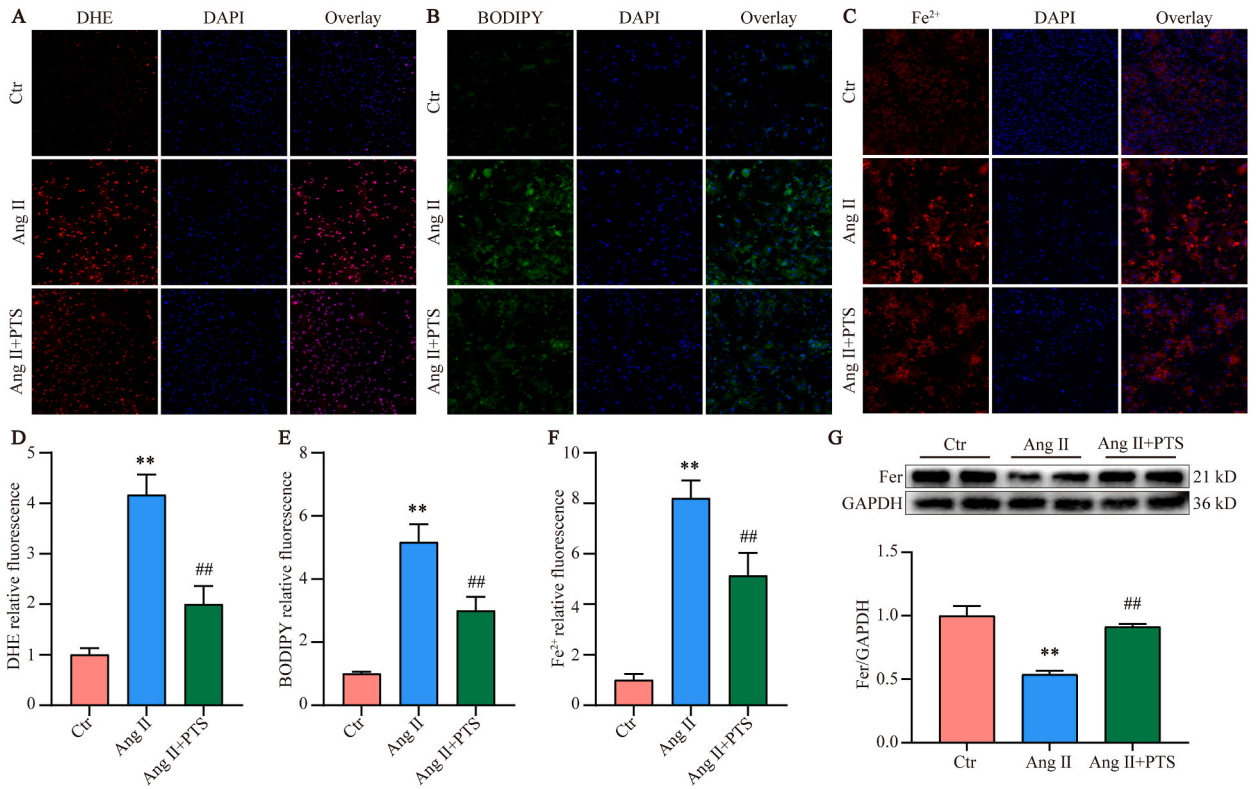

Fig. 1. PTS rescues Ang II-induced increases in ferroptosis in cultured myocardial cells. (A–F) PTS reduced ROS (200 ×), lipid peroxides (200 ×) and Fe^{2+} (200 ×) levels in CMs. (G) Western blot analysis exhibited decrease ferritin in H9C2 cells in response to Ang II, which can be rescued by PTS. n ≥ 3 in all cell experiments, $^{**}P < 0.01$ versus the control group; $^{\#\#}P < 0.01$ versus the Ang II group. DHE, dihydroethidium; Ctr, control; Ang II, angiontensin II; PTS, pterostilbene; Fer, ferritin; GAPDH, glyceraldehyde -3-phosphate dehydrogenase.

was added to the cell culture plate and placed into the incubator, and the medium was replaced with fresh medium after 4–6 h.

2.9. Assays of intracellular lipid peroxidation, ROS and Fe^{2+}

CMs were inoculated in six-well plates. After a certain period of time, washing them with PBS. Then CMs were incubated with C11-BODIPY581/591 9 (#D3861, Thermo Fisher Scientific, USA), FerroOrange (#F374, Dojndo, Japan) or dihydroethidium (DHE, #S0033S-1, Beyotime, China) regent respectively for 30 min. Washed again with PBS and the cells were visualized by fluorescence microscopy.

2.10. Biochemical assay kits

Accordance with the manufacturer's instructions, cardiac MDA level were measured using MDA Assay (#ab118970, Abcam, USA) Kit.

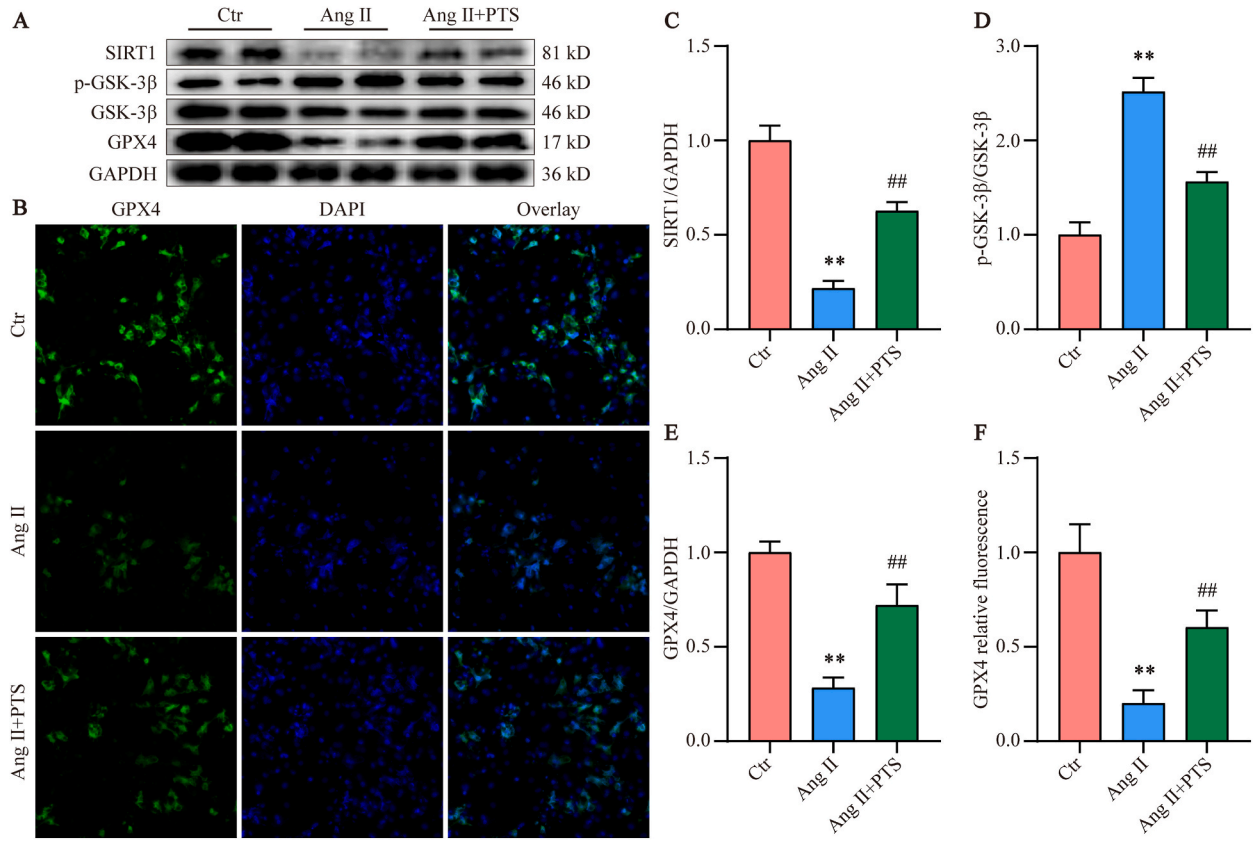

Fig. 2. PTS prevents against cardiac ferroptosis by SIRT1/GSK-3β/GPX4 signaling. (A, C-E) Representative Western blot images and quantitative analysis of SIRT1, GSK-3β, p-GSK-3β, and GPX4 in H9C2 cells. (B, F) Immunofluorescence staining reveals decreased GPX4 expression in Ang II-induced CMs, which is rescued by PTS. n ≥ 3 in all cell experiments, $^{**}P < 0.01$ versus the control group; $^{\#\#}P < 0.01$ versus the Ang II group. Ctr, control; Ang II, angiontensin II; PTS, pterostilbene; SIRT1, sirtuin 1; GSK-3β, glycogen synthase kinase-3β; p-GSK-3β, phosphorylation of glycogen synthase kinase-3β; GPX4, glutathione peroxidase 4; GAPDH, glyceraldehyde -3-phosphate dehydrogenase.

2.11. Western blot analysis

Using RIPA buffer (#P0013B, Beyotime, Shanghai, China) to lyse heart tissue or CMs and obtain proteins in samples, and detecting Protein Concentration with BCA Protein Assay Kit (#23227, Thermo Fisher Scientific, Massachusetts, USA). Expression levels of specific proteins in equal amount samples were detected by electrophoresis. The steps are as follows. Proteins were added to each well of the SDS-PAGE gel (#PG212, Epizyme Biomedical Technology Co. Ltd., Shanghai, China) in a specific order. Electrophoresis was performed and the proteins were then transferred to a PVDF membrane (#03010040001, Roche, Basel, Switzerland). Blocking the membrane in 5 % skimmed milk (#BS102, Biosharp Co. Ltd., Chengdu, China) for 1.5 h and washing them three times with tris-buffered saline-Tween (TBST). The membranes were incubated with primary antibody dilutions at 4 °C overnight. On the next day, the membrane was washed with TBST again for 3 times, and then incubated with the secondary antibody dilution for 2 h at room temperature. Using ECL substrate (#SQ201, Epizyme Biomedical Technology Co. Ltd., Shanghai, China) to exposure PVDF membranes. Image J software was used to analyze the intensity of blots. All antibodies used in this experiment are listed in Table 1.

2.12. Statistical analysis

For all animal experiments, n ≥ 6, while cell experiments contained n ≥ 3. Independent repeated experiments were performed at least in triplicate. SPSS 26.0 software was used for statistical analysis and data are shown as mean ± standard error (SEM). Student's t-test was performed to assess differences between two groups and one way analysis of variance (ANOVA) followed by Tukey's HSD multiple comparison post-hoc test was used for multiple groups. $P < 0.05$ was considered statistically significant.

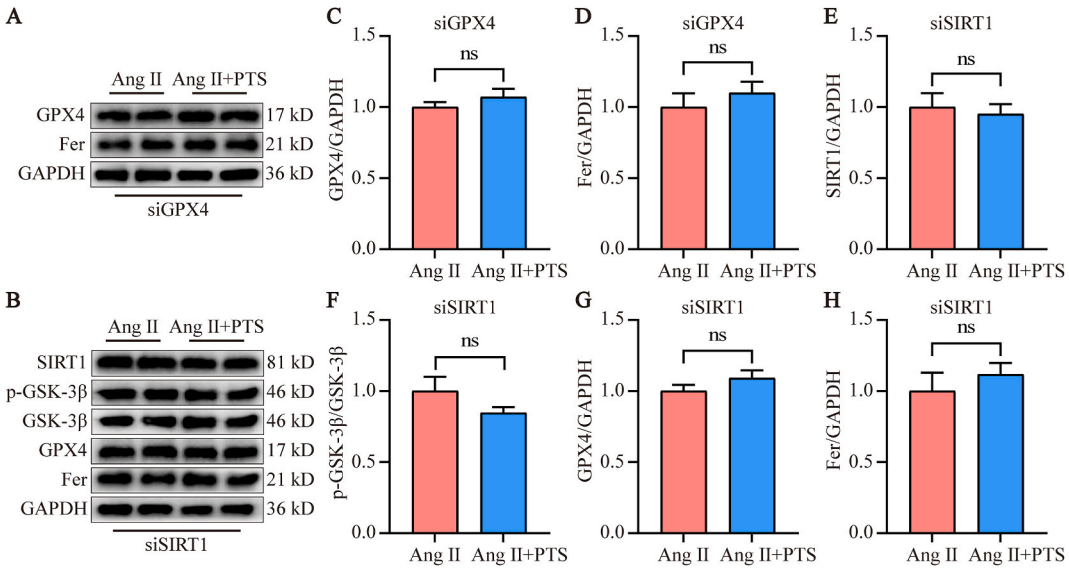

Fig. 3. GPX4 or Sirt1 knockdown mitigated the effects of PTS in CMs. (A) siGPX4 took away the protective effect of PTS on cardiomyocytes. (B) Western blot results show the expressions of SITR1, p-GSK-3β, GSK-3β, GPX4, and ferritin in SIRT1 knockdown cardiomyocytes. n ≥ 3 in all cell experiments, ns $P \geq 0.05$. Ang II, angiontensin II; PTS, pterostilbene; SIRT1, sirtuin 1; GSK-3β, glycogen synthase kinase-3β; p-GSK-3β, phosphorylation of glycogen synthase kinase-3β; GPX4, glutathione peroxidase 4; Fer, ferritin; GAPDH, glyceraldehyde -3-phosphate dehydrogenase.

3. Results

3.1. PTS alleviates Ang II-induced ferroptosis in cardiomyocytes

The production of ROS and lipid peroxidases is a hallmark of ferroptosis. Accumulation of reduced ferrous iron (Fe^{2+}) is an early signal initiating ferroptosis. Ferritin (Fer) is a major intracellular iron storage protein, and its expression limits ferroptosis. To verify whether PTS affects cardiomyocyte ferroptosis, we used Ang II to stimulate CMs and evaluated the effects of PTS on ROS production, lipid peroxidation, and Fe^{2+} levels. Intracellular ROS and oxidized lipids increased in CMs treated with Ang II for 48 h. Compared to Ang II, PTS treatment reduced the enrichment of intracellular ROS and lipid peroxides (Fig. 1A–B and D-E). PTS also reduced the Ang II-induced accumulation of Fe^{2+} and increased the expression of ferritin (Fig. 1C and F-G). Collectively, these results suggest that PTS alleviates ferroptosis in cardiomyocytes (see Fig. 1).

3.2. PTS inhibits Ang II-induced cardiomyocyte ferroptosis through SIRT1/GSK-3β signaling pathway

The activated SIRT1/GSK-3β/GPX4 pathway plays an important role in ferroptosis. To determine whether PTS exerted effects through the SIRT1/GSK-3β/GPX4 pathway, we examined the expression of SIRT1, GSK-3β, p-GSK-3β, and GPX4 in myocardial cells after stimulation by Ang II. Immunofluorescence results suggested that the expression of GPX4 in the CMs was significantly decreased (Fig. 2B and F). PTS treatment markedly increased GPX4 expression, and Western blot analysis revealed the same trend. In addition, the expression of SIRT1 decreased and that of p-GSK-3β was increased in myocardial cells treated with Ang II (Fig. 2A and C-E). However, PTS treatment delayed this change.

3.3. Knockdown of SIRT1 or GPX4 mitigated the effects of PTS in H9C2 cells

To further explore the signaling pathways through which PTS inhibits ferroptosis in myocardial cells, siRNAs were designed. We observed that the inhibitory effect of PTS on cardiomyocyte ferroptosis was abolished by blocking the expression of GPX4, a key protein involved in ferroptosis (Fig. 3A and C-D). Blocking the SIRT1 pathway significantly attenuated the inhibitory effect of PTS on myocardial ferroptosis via the SITR1/GSK-3β/GPX4 pathway (Fig. 3B and E-H). Based on these results, we deduced that the inhibitory effect of PTS on cardiomyocyte ferroptosis occurs mainly through the SITR1/GSK-3β/GPX4 pathway.

3.4. PTS alleviated pressure overload-induced ventricular systolic dysfunction in mice

For the *in vitro* experiments, we constructed a TAC mouse model to examine the potential cardioprotective effects of PTS on HF. Wild-type (WT) mice were treated with PTS (50 mg/kg) for eight weeks after TAC. We observed a significant decrease in cardiac function in TAC mice, as shown by reduced left ventricular ejection fraction (LVEF%), fractional shortening (LVFS%), and cardiac index (CO), as well as increased left ventricular internal dimensions at systole (LVIDs) and left ventricular internal dimensions at

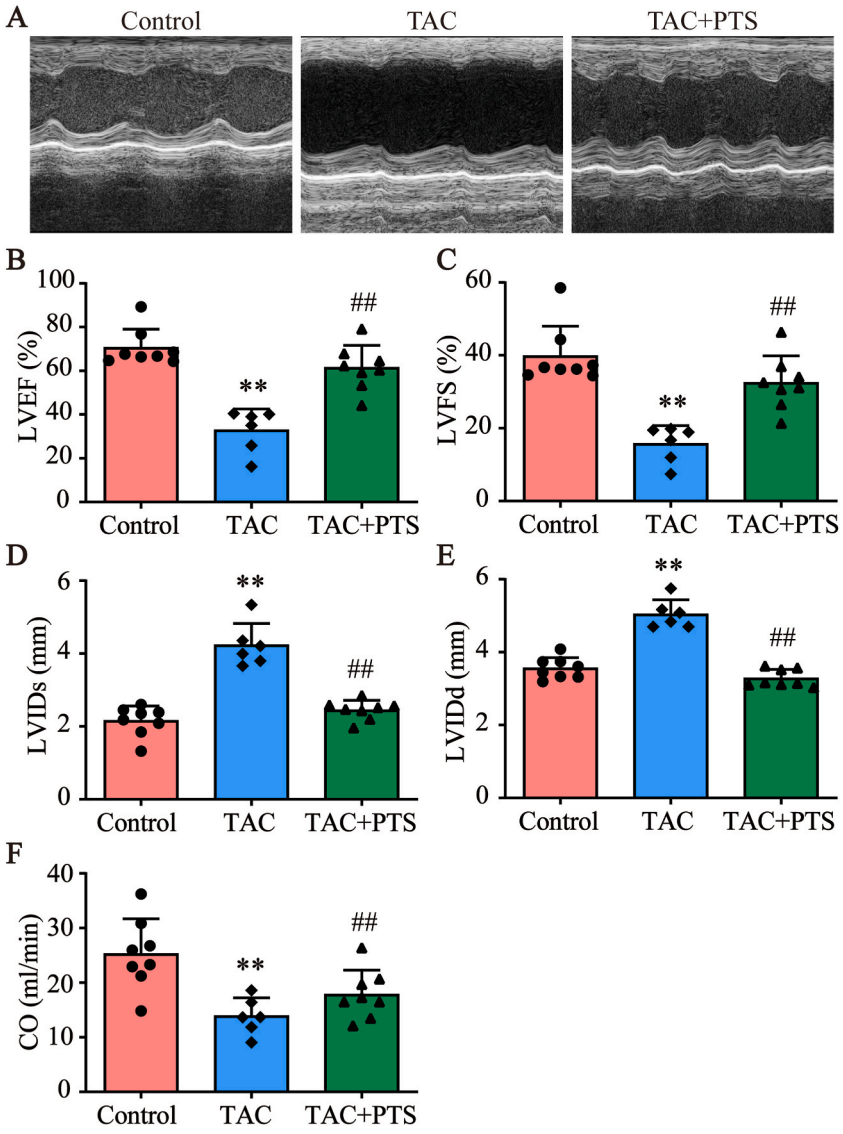

Fig. 4. PTS rescued impaired cardiac function in mice after TAC. (A) Representative images of cardiac echocardiography in each group. The parameters detected by echocardiography displayed by a bar graph: (B) left ventricular ejection fraction (LVEF%); (C) fractional shortening (LVFS%); (D) left ventricular internal dimensions at systole (LVIDs); (E) left ventricular internal dimensions at diastole (LVIDd); (F) cardiac index (CO). $n \geq 6$ in all animal experiments, $^{**}P < 0.01$ versus the control group; $^{\#\#}P < 0.01$ versus the TAC group. TAC, transverse aortic constriction; PTS, pterostilbene.

diastole (LVIDd). However, PTS treatment prevented HF, as evidenced by an increase in EF%, FS%, and CO, and a decrease in LVID (Fig. 4). These results demonstrate that PTS suppresses ventricular systolic dysfunction in mice with pressure overload, suggesting that PTS may protect against hypertension-mediated cardiac injury.

3.5. PTS alleviated the pathological cardiac remodeling

We further evaluated the effects of PTS on cardiac hypertrophy and fibrosis. PTS rescued the increased HW/BW ratio and HW/TL ratio in mice after TAC (Fig. 5C and D). Myocardial cell size, which was significantly increased in TAC mouse hearts, was also reduced by PTS. In the histological analysis, H&E and WGA staining showed that TAC-induced cardiomyocyte hypertrophy was reversed by PTS (Fig. 5A–B and F). PTS treatment significantly reduced the cardiac collagen volume fraction (Fig. 5 A-B and E). In summary, PTS remarkably alleviated cardiac remodeling.

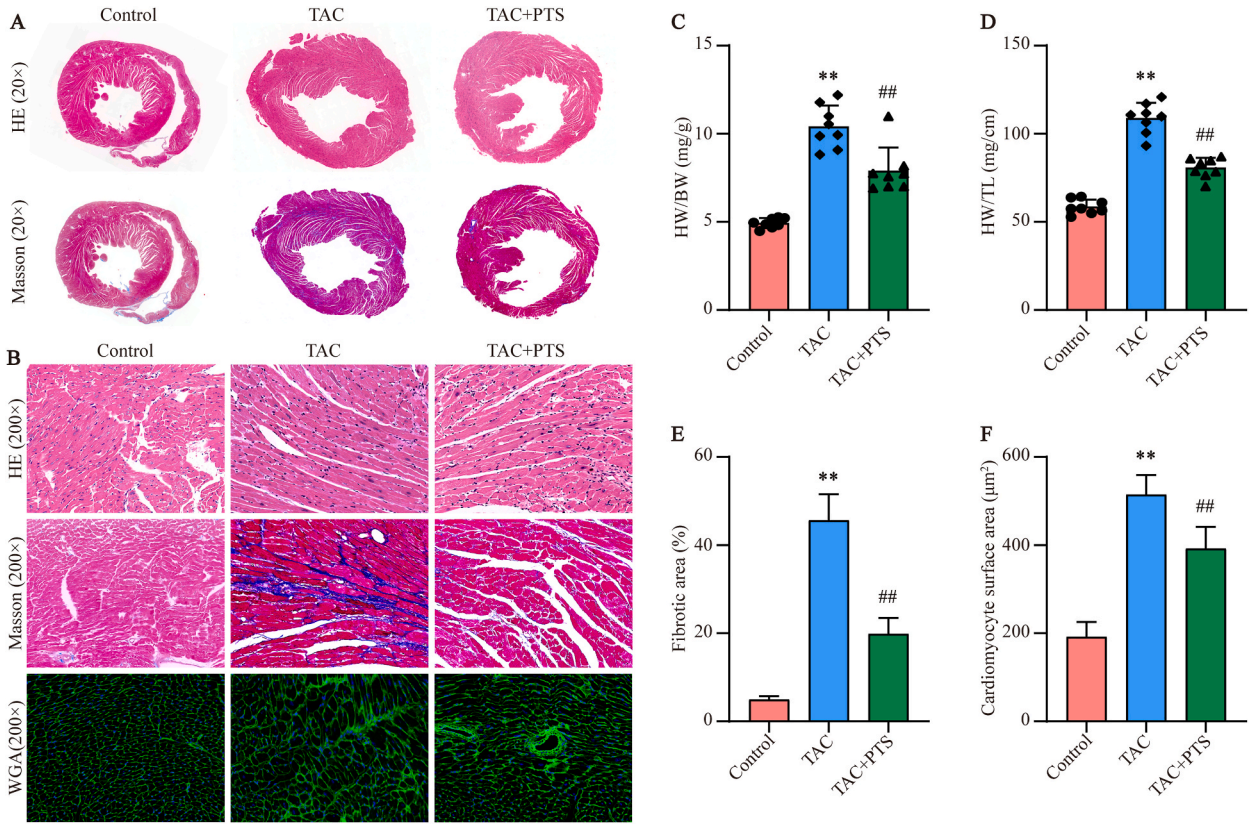

Fig. 5. PTS inhibited myocardial damage in heart failure. (A) H&E and Masson's staining (20 ×) for assessment of myocardial injury after TAC. (B) Representative H&E, Masson's and WGA staining images (200 ×) in each groups. (C, D) HW/BW ratio and HW/TL ratio in the different groups. (E, F) Quantification of the fibrotic area and cardiomyocyte hypertrophy in mice. n ≥ 6 in all animal experiments, $^{**}P < 0.01$ versus the control group; $^{\#\#}P < 0.01$ versus the TAC group. HE, haematoxylin and eosin; TAC, transverse aortic constriction; PTS, pterostilbene; HW, heart weight; BW, body weight; TL, tibia length; WGA, wheat germ agglutinin.

3.6. PTS reduces cardiomyocyte ferroptosis through the SIRT1/GSK-3β/GPX4 pathway in mice after TAC

In order to study the preventive effect and mechanism of PTS on myocardial ferroptosis in HF mice, the expression of GPX4 and related regulatory pathway SIRT1/GSK-3β was detected by immunofluorescence and Western blot (Fig. 6). In this work, treatment of mice with PTS after TAC was linked with upregulation of SIRT1 and GPX4 and downregulation of p-GSK-3β. These results are consistent with those of the *in vitro* experiments.

3.7. Cardiomyocyte ferroptosis occurred in mice after TAC, which can be alleviated by PTS

Furthermore, to explore whether PTS exerts cardioprotective effects by affecting cardiomyocyte ferroptosis in HF mice, we constructed a TAC mouse model for *in vitro* experiments. Ferroptosis is accompanied by ROS production. Mitochondria are the major organelles responsible for cellular ROS generation; thus, ferroptosis is usually accompanied by changes in the mitochondrial structure. To explore whether PTS exerts cardioprotective effects by affecting cardiomyocyte ferroptosis in mice, we used TEM, immunofluorescence, and Western blot to detect mitochondrial damage, oxidative stress and ferritin expression, which were involved in ferroptosis. After TAC, mouse cardiomyocytes had smaller mitochondria, reduced or absent mitochondrial cristae, and condensed mitochondrial membrane density, whereas PTS attenuated mitochondrial morphological abnormalities and cell death (Fig. 7A). Immunofluorescence and Western blot showed that ROS levels increased and ferritin expression decreased in myocardial tissue after TAC. However, PTS treatment significantly attenuated these effects (Fig. 7B–E). We conclude that PTS attenuates ferroptosis in mice with HF.

4. Discussion

HF is the end stage of various heart diseases and is primarily caused by hypertension, myocardial infarction, and degenerative valve disease, etc. It has high morbidity and mortality rates worldwide [39]. Pressure overload-induced HF is usually accompanied by the loss of myocytes and adverse changes in the surviving myocytes and extracellular matrix, including myocardial hypertrophy and

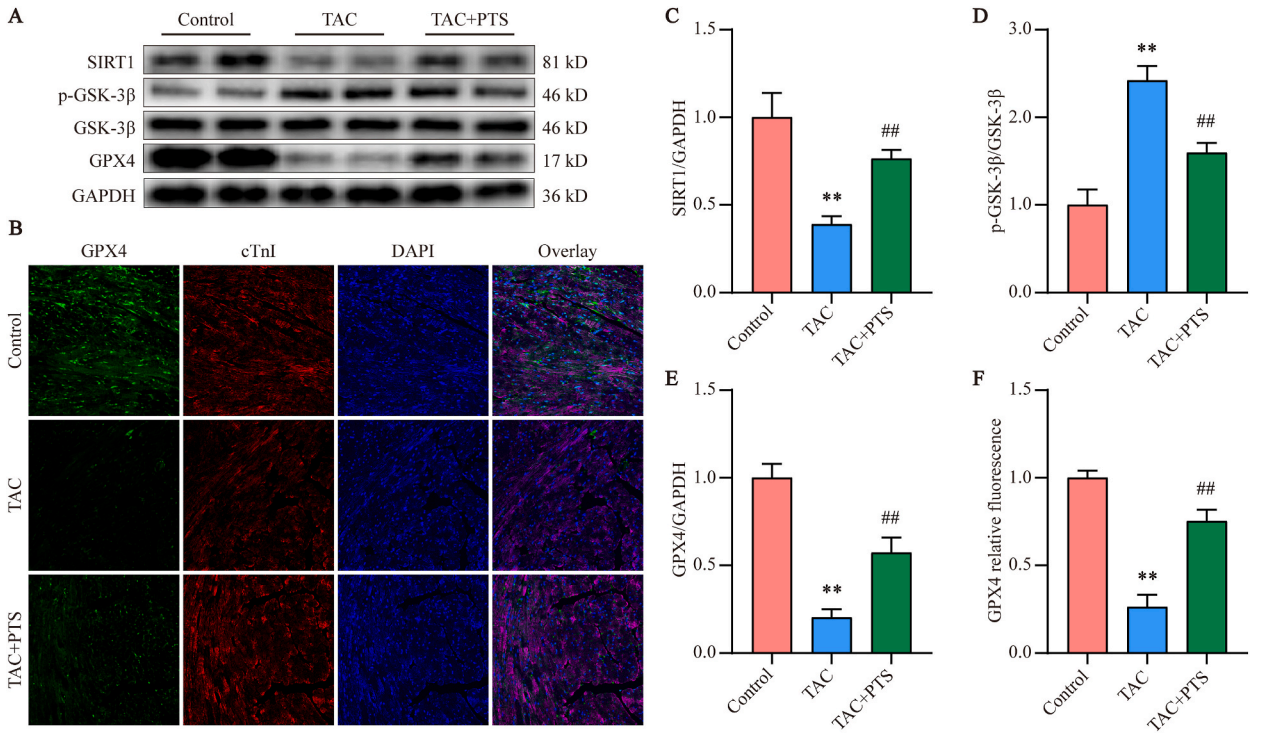

Fig. 6. PTS influenced SIRT1/GSK-3β/GPX4 pathway in mice. (A, C-E) Western blot analysis of SIRT1, p-GSK-3β, GSK-3β, GPX4 protein expressions in each group. (B, F) Immunofluorescence staining reveals relative expression of GPX4 in mouse myocardial tissue in each group. n ≥ 6 in all animal experiments, $^{**}P < 0.01$ versus the control group; $^{\#\#}P < 0.01$ versus the TAC group. TAC, transverse aortic constriction; PTS, pterostilbene; SIRT1, sirtuin 1; GSK-3β, glycogen synthase kinase-3β; p-GSK-3β, phosphorylation of glycogen synthase kinase-3β; GPX4, glutathione peroxidase 4; GAPDH, glyceraldehyde -3-phosphate dehydrogenase.

cardiac fibrosis [40,41]. Owing to hemodynamic changes, the functions of other organs such as the lungs, liver, kidneys, and blood vessels are also impaired, resulting in a vicious systemic pathophysiological cycle.

Ferroptosis plays a crucial role in the pathophysiology of various cardiovascular diseases [42,43]. Several studies have shown that cardiomyocytes are highly susceptible to free iron overload [44–46]. Cardiac ferritin levels are important indicators of cardiac function [42]. Iron in ferritin is released as free iron during ferroptosis, and excessive iron loading can further aggravate myocardial injury. Therefore, in the present study, we focused on inhibiting cardiomyocyte ferroptosis to alleviate the development of HF and ventricular remodeling.

The PTS was found to have an excellent ability to resist oxidative stress. In addition, in a study on liver fibrosis, PTS was found to inhibit the increase in collagen 1 [47]. However, whether PTS regulates cardiomyocyte ferroptosis has not yet been investigated. In this study, we demonstrated for the first time that PTS protects against cardiomyocyte ferroptosis and, consequently, against HF and cardiac remodeling.

Ferroptosis is a form of cell death characterized by an iron overload that results in the accumulation of ROS and lipid peroxides. High iron levels can cause severe cardiac injury, which can be rescued by a ferroptosis inhibitor Fer-1. Our study indicated that there was an increase in iron and MDA levels in mouse hearts with HF, leading to the upregulation of ROS, which was reversed by PTS. Therefore, we propose that PTS negatively regulates cardiac ferroptosis in hypertensive HF. Additionally, decreased iron storage leads to iron overload during ferroptosis [48]. We demonstrated that PTS rescued the reduced ferritin levels and increased ROS and lipid peroxides in cultured myocardial cells treated with Ang II. These findings strongly suggest that PTS has therapeutic potential for the prevention and treatment of cardiac ferroptosis in the heart.

SIRT1 activity has been implicated in the prevention of ferroptosis [49]. Inhibition of SIRT1 activity induces HF [50]. GSK-3β is closely associated with myocardial cell death and cardiac fibrosis [51]. Consistent with this, we found that PTS prevented heart ferroptosis and significantly elevated the expression of SIRT1. Overexpression of SIRT1 can regulate p-GSK-3β expression, subsequently elevating GPX4, which was inactivated in the TAC hearts or Ang II-stimulated myocardial cells. We then designed siRNAs to knockdown GPX4 in myocardial cells, and the regulatory effect of PTS on ferritin almost disappeared. Similarly, when SIRT1 was knocked down, the effect of PTS on p-GSK-3β and GPX4 expression was subsequently abolished. These results suggest that PTS modulates cardiomyocyte ferroptosis via the SIRT1/GSK-3β/GPX4 pathway. They also imply that other SIRT1 regulatory drugs or treatments may exert the same cardioprotective effect. In the future, more studies are needed to confirm this conjecture and provide new ideas for the treatment of heart failure.

Our findings should be interpreted in the context of several limitations. Despite the representative features of *in vitro* experiments, it

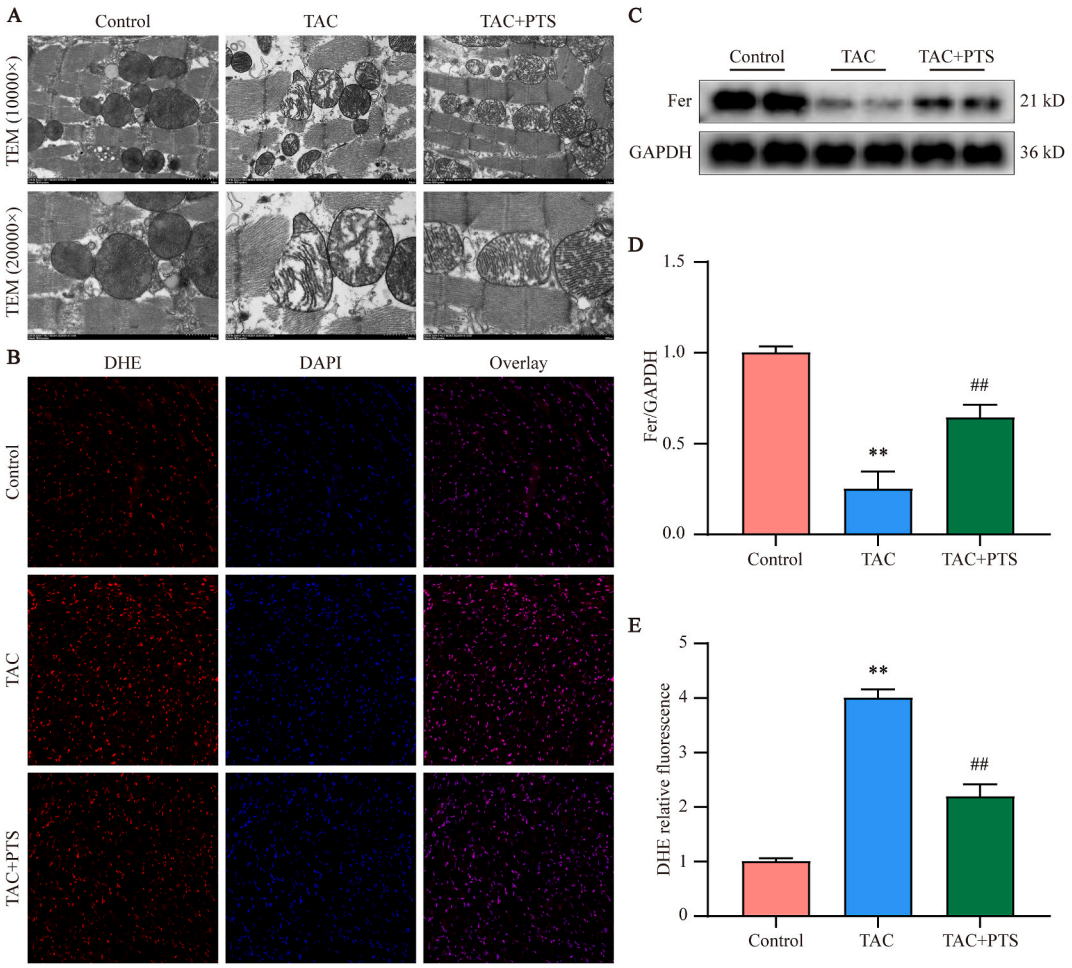

Fig. 7. PTS attenuates cardiac ferroptosis *in vivo*. (A) TEM images for cardiac tissue in each group. (B, E) DHE staining shows that PTS restores TAC-induced ROS generation in heart failure. (C, D) The Fer expression was determined by Western blot. n ≥ 6 in all animal experiments, $^{**}P < 0.01$ versus the control group; $^{\#\#}P < 0.01$ versus the TAC group. TAC, transverse aortic constriction; PTS, pterostilbene; TEM, transmission electron microscope; Fer, ferritin; GAPDH, glyceraldehyde -3-phosphate dehydrogenase; DHE, dihydroethidium.

would be better to evaluate the mechanism of PTS in a more nuanced manner in an *in vivo* model. HF is not only closely related to cardiomyocyte ferroptosis but also to a variety of physiological and pathological processes, including inflammation, autophagy, and pyroptosis. Additionally, the dysfunction of fibroblasts, immune cells, endothelial cells, and smooth muscle cells may affect the pathological progression of HF. All of these factors potentially play important roles in PTS-induced cardioprotection. However, the present study focused mainly on cardiomyocyte ferroptosis to confirm the effects of the PTS on HF. Despite our finding that the PTS works well, these results cannot be translated into clinical practice. Further clinical trials are required for a better clinical translation.

5. Conclusion

This study revealed that the expression of SIRT1 is downregulated in the hearts of mice with HF, which was related to cardiomyocyte ferroptosis, pathological hypertrophy, myocardial fibrosis, and dysfunction. PTS effectively hindered this trend and ferroptosis in HF, thus improving heart function and alleviating cardiac remodeling. Notably, SIRT1 activation results in a reduction of p-GSK-3β while attenuating GPX4 deficiency in HF, ultimately inhibiting ferroptosis. The *in vivo* and *in vitro* data delineate the important role of PTS in HF. This discovery provides new ideas for the prevention of HF.

Data availability

No data was used for the research described in the article.

Additional information

No additional information is available for this paper.

CRediT authorship contribution statement

Fan Zhang: Writing – original draft, Validation, Methodology, Investigation, Formal analysis, Conceptualization. **Zhuanglin Zeng:** Visualization, Validation, Investigation, Formal analysis. **Jiahui Zhang:** Validation, Investigation, Formal analysis. **Xuelian Li:** Validation, Investigation, Formal analysis. **Wenling Yang:** Validation, Investigation, Formal analysis. **Yumiao Wei:** Writing – review & editing, Validation, Supervision, Resources. **Xiaopeng Guo:** Writing – review & editing, Visualization, Validation, Resources, Formal analysis.

Declaration of competing interest

The authors declare the following financial interests/personal relationships which may be considered as potential competing interests:Xiaopeng Guo reports financial support was provided by National Natural Science Foundation of China. Yumiao Wei reports financial support was provided by National Natural Science Foundation of China. If there are other authors, they declare that they have no known competing financial interests or personal relationships that could have appeared to influence the work reported in this paper.

Acknowledgements

This work was supported by grants of the National Natural Science Foundation of China (Grant number: 82202281, 82070376 and 81873491). Graphical Abstract have been created with BioRender.com.

Appendix A. Supplementary data

Supplementary data to this article can be found online at https://doi.org/10.1016/j.heliyon.2024.e24562.

References

[1] N.L. Bragazzi, W. Zhong, J. Shu, A. Abu Much, D. Lotan, A. Grupper, A. Younis, H. Dai, Burden of heart failure and underlying causes in 195 countries and territories from 1990 to 2017, European J. Prevent. Cardiol. 28 (15) (2021) 1682–1690.
[2] E. Shahar, S. Lee, J. Kim, S. Duval, C. Barber, R.V. Luepker, Hospitalized heart failure: rates and long-term mortality, J. Card. Fail. 10 (5) (2004) 374–379.
[3] K.S. Shah, H. Xu, R.A. Matsouaka, D.L. Bhatt, P.A. Heidenreich, A.F. Hernandez, A.D. Devore, C.W. Yancy, G.C. Fonarow, Heart failure with preserved, borderline, and reduced ejection fraction: 5-year outcomes, J. Am. Coll. Cardiol. 70 (20) (2017) 2476–2486.
[4] F. Bazgir, J. Nau, S. Nakhaei-Rad, E. Amin, M.J. Wolf, J.J. Saucerman, K. Lorenz, M.R. Ahmadian, The microenvironment of the pathogenesis of cardiac hypertrophy, Cells 12 (13) (2023) 1780.
[5] P.K. Baffour, L. Jahangiry, S. Jain, A. Sen, D. Aune, Blood pressure, hypertension and the risk of heart failure: a systematic review and meta-analysis of cohort studies, European J. Prevent. Cardiol. (2023).
[6] V. Kamperidis, V. Delgado, N.M. van Mieghem, A.P. Kappetein, M.B. Leon, J.J. Bax, Diagnosis and management of aortic valve stenosis in patients with heart failure, Eur. J. Heart Fail. 18 (5) (2016) 469–481.
[7] K.E. Di Palo, N.J. Barone, Hypertension and heart failure: prevention, targets, and treatment, Heart Fail. Clin. 16 (1) (2020) 99–106.
[8] L. Guariguata, D.R. Whiting, I. Hambleton, J. Beagley, U. Linnenkamp, J.E. Shaw, Global estimates of diabetes prevalence for 2013 and projections for 2035, Diabetes Res. Clin. Pract. 103 (2) (2014) 137–149.
[9] E. Tanai, S. Frantz, Pathophysiology of heart failure, Compr. Physiol. 6 (1) (2015) 187–214.
[10] A. van der Pol, W.H. van Gilst, A.A. Voors, P. van der Meer, Treating oxidative stress in heart failure: past, present and future, Eur. J. Heart Fail. 21 (4) (2019) 425–435.
[11] S.J. Dixon, K.M. Lemberg, M.R. Lamprecht, R. Skouta, E.M. Zaitsev, C.E. Gleason, D.N. Patel, A.J. Bauer, A.M. Cantley, W.S. Yang, B. Morrison 3rd, B. R. Stockwell, Ferroptosis: an iron-dependent form of nonapoptotic cell death, Cell 149 (5) (2012) 1060–1072.
[12] D. Liang, A.M. Minikes, X. Jiang, Ferroptosis at the intersection of lipid metabolism and cellular signaling, Mol. Cell 82 (12) (2022) 2215–2227.
[13] C. Du, L. Zhou, J. Qian, M. He, Z.G. Zhang, C. Feng, Y. Zhang, R. Zhang, C.M. Dong, Ultrasmall zwitterionic polypeptide-coordinated nanohybrids for highly efficient cancer photothermal ferrotherapy, ACS Appl. Mater. Interfaces 13 (37) (2021) 44002–44012.
[14] K. Bersuker, J.M. Hendricks, Z. Li, L. Magtanong, B. Ford, P.H. Tang, M.A. Roberts, B. Tong, T.J. Maimone, R. Zoncu, M.C. Bassik, D.K. Nomura, S.J. Dixon, J. A. Olzmann, The CoQ oxidoreductase FSP1 acts parallel to GPX4 to inhibit ferroptosis, Nature 575 (7784) (2019) 688–692.
[15] J.P. Friedmann Angeli, M. Schneider, B. Proneth, Y.Y. Tyurina, V.A. Tyurin, V.J. Hammond, N. Herbach, M. Aichler, A. Walch, E. Eggenhofer, D. Basavarajappa, O. Rådmark, S. Kobayashi, T. Seibt, H. Beck, F. Neff, I. Esposito, R. Wanke, H. Förster, O. Yefremova, M. Heinrichmeyer, G.W. Bornkamm, E.K. Geissler, S. B. Thomas, B.R. Stockwell, V.B. O'Donnell, V.E. Kagan, J.A. Schick, M. Conrad, Inactivation of the ferroptosis regulator Gpx4 triggers acute renal failure in mice, Nat. Cell Biol. 16 (12) (2014) 1180–1191.
[16] D.P. Del Re, D. Amgalan, A. Linkermann, Q. Liu, R.N. Kitsis, Fundamental mechanisms of regulated cell death and implications for heart disease, Physiol. Rev. 99 (4) (2019) 1765–1817.
[17] Z. Zhang, J. Tang, J. Song, M. Xie, Y. Liu, Z. Dong, X. Liu, X. Li, M. Zhang, Y. Chen, H. Shi, J. Zhong, Elabela alleviates ferroptosis, myocardial remodeling, fibrosis and heart dysfunction in hypertensive mice by modulating the IL-6/STAT3/GPX4 signaling, Free Radic. Biol. Med. 181 (2022) 130–142.
[18] J. Wang, B. Deng, Q. Liu, Y. Huang, W. Chen, J. Li, Z. Zhou, L. Zhang, B. Liang, J. He, Z. Chen, C. Yan, Z. Yang, S. Xian, L. Wang, Pyroptosis and ferroptosis induced by mixed lineage kinase 3 (MLK3) signaling in cardiomyocytes are essential for myocardial fibrosis in response to pressure overload, Cell Death Dis. 11 (7) (2020) 574.

[19] H. Esterbauer, R.J. Schaur, H. Zollner, Chemistry and biochemistry of 4-hydroxynonenal, malonaldehyde and related aldehydes, Free Radic. Biol. Med. 11 (1) (1991) 81–128.
[20] Z. Zhou, T.J. Ye, E. DeCaro, B. Buehler, Z. Stahl, G. Bonavita, M. Daniels, M. You, Intestinal SIRT1 deficiency protects mice from ethanol-induced liver injury by mitigating ferroptosis, Am. J. Pathol. 190 (1) (2020) 82–92.
[21] Z. Qiongyue, Y. Xin, P. Meng, M. Sulin, W. Yanlin, L. Xinyi, S. Xuemin, Post-treatment with irisin attenuates acute kidney injury in sepsis mice through anti-ferroptosis via the SIRT1/Nrf2 pathway, Front. Pharmacol. 13 (2022) 857067.
[22] M. Packer, Cardioprotective effects of sirtuin-1 and its downstream effectors: potential role in mediating the heart failure benefits of SGLT2 (Sodium-Glucose cotransporter 2) inhibitors, circulation, Heart Fail. 13 (9) (2020) e007197.
[23] A. Prola, J. Pires Da Silva, A. Guilbert, L. Lecru, J. Piquereau, M. Ribeiro, P. Mateo, M. Gressette, D. Fortin, C. Boursier, C. Gallerne, A. Caillard, J.L. Samuel, H. François, D.A. Sinclair, P. Eid, R. Ventura-Clapier, A. Garnier, C. Lemaire, SIRT1 protects the heart from ER stress-induced cell death through eIF2α deacetylation, Cell Death Differ. 24 (2) (2017) 343–356.
[24] P.P. Su, D.W. Liu, S.J. Zhou, H. Chen, X.M. Wu, Z.S. Liu, Down-regulation of Risa improves podocyte injury by enhancing autophagy in diabetic nephropathy, Milit. Medical Res. 9 (1) (2022) 23.
[25] J. Lin, T. Song, C. Li, W. Mao, GSK-3β in DNA repair, apoptosis, and resistance of chemotherapy, radiotherapy of cancer, Biochimica et biophysica acta, Molecular Cell Res. 1867 (5) (2020) 118659.
[26] O.H.M. Elmadbouh, S.J. Pandol, M. Edderkaoui, Glycogen synthase kinase 3β: a true foe in pancreatic cancer, Int. J. Mol. Sci. 23 (22) (2022) 14133.
[27] Z. Li, H. Zhu, C. Liu, Y. Wang, D. Wang, H. Liu, W. Cao, Y. Hu, Q. Lin, C. Tong, M. Lu, A. Sachinidis, L. Li, L. Peng, GSK-3β inhibition protects the rat heart from the lipopolysaccharide-induced inflammation injury via suppressing FOXO3A activity, J. Cell Mol. Med. 23 (11) (2019) 7796–7809.
[28] X. Jiang, J. Zhou, Y. Wang, X. Liu, K. Xu, J. Xu, F. Feng, H. Sun, PROTACs suppression of GSK-3β, a crucial kinase in neurodegenerative diseases, Eur. J. Med. Chem. 210 (2021) 112949.
[29] M.J. Stachowski-Doll, M. Papadaki, T.G. Martin, W. Ma, H.M. Gong, S. Shao, S. Shen, N.A. Muntu, M. Kumar, E. Perez, J.L. Martin, C.S. Moravec, S. Sadayappan, S.G. Campbell, T. Irving, J.A. Kirk, GSK-3β localizes to the cardiac Z-disc to maintain length dependent activation, Circ. Res. 130 (6) (2022) 871–886.
[30] S.H. Wang, L.G. Cui, X.L. Su, S. Komal, R.C. Ni, M.X. Zang, L.R. Zhang, S.N. Han, GSK-3β-mediated activation of NLRP3 inflammasome leads to pyroptosis and apoptosis of rat cardiomyocytes and fibroblasts, Eur. J. Pharmacol. 920 (2022) 174830.
[31] Z. Cui, X. Zhao, F.K. Amevor, X. Du, Y. Wang, D. Li, G. Shu, Y. Tian, X. Zhao, Therapeutic application of quercetin in aging-related diseases: SIRT1 as a potential mechanism, Front. Immunol. 13 (2022) 943321.
[32] Y. Yang, J. Wang, Y. Li, C. Fan, S. Jiang, L. Zhao, S. Di, Z. Xin, B. Wang, G. Wu, X. Li, Z. Li, X. Gao, Y. Dong, Y. Qu, HO-1 signaling activation by pterostilbene treatment attenuates mitochondrial oxidative damage induced by cerebral ischemia reperfusion injury, Mol. Neurobiol. 53 (4) (2016) 2339–2353.
[33] H. Liu, L. Zhao, L. Yue, B. Wang, X. Li, H. Guo, Y. Ma, C. Yao, L. Gao, J. Deng, L. Li, D. Feng, Y. Qu, Pterostilbene attenuates early brain injury following subarachnoid hemorrhage via inhibition of the NLRP3 inflammasome and Nox2-related oxidative stress, Mol. Neurobiol. 54 (8) (2017) 5928–5940.
[34] Y.C. Hseu, Y. Vudhya Gowrisankar, L.W. Wang, Y.Z. Zhang, X.Z. Chen, P.J. Huang, H.R. Yen, H.L. Yang, The in vitro and in vivo depigmenting activity of pterostilbene through induction of autophagy in melanocytes and inhibition of UVA-irradiated α-MSH in keratinocytes via Nrf2-mediated antioxidant pathways, Redox Biol. 44 (2021) 102007.
[35] X. Yang, Z. Liu, M. Fang, T. Zou, Z. Zhang, X. Meng, T. Wang, H. Meng, Y. Chen, Y. Duan, Q. Li, Novel pterostilbene derivatives ameliorate heart failure by reducing oxidative stress and inflammation through regulating Nrf2/NF-κB signaling pathway, Eur. J. Med. Chem. 258 (2023) 115602.
[36] D. Lacerda, P. Türck, C. Campos-Carraro, A. Hickmann, V. Ortiz, S. Bianchi, A. Belló-Klein, A.L. de Castro, V.L. Bassani, A. Araujo, Pterostilbene improves cardiac function in a rat model of right heart failure through modulation of calcium handling proteins and oxidative stress, Appl. Physiol. Nutrit. Metabolism = Physiologie Appliquee, Nutrition et metabolisme 45 (9) (2020) 987–995.
[37] L. Song, T.Y. Chen, X.J. Zhao, Q. Xu, R.Q. Jiao, J.M. Li, L.D. Kong, Pterostilbene prevents hepatocyte epithelial-mesenchymal transition in fructose-induced liver fibrosis through suppressing miR-34a/Sirt1/p53 and TGF-β1/Smads signalling, Br. J. Pharmacol. 176 (11) (2019) 1619–1634.
[38] Y. Chen, H. Zhang, S. Ji, P. Jia, Y. Chen, Y. Li, T. Wang, Resveratrol and its derivative pterostilbene attenuate oxidative stress-induced intestinal injury by improving mitochondrial redox homeostasis and function via SIRT1 signaling, Free Radic. Biol. Med. 177 (2021) 1–14.
[39] J.J. McMurray, M.A. Pfeffer, Heart failure, Lancet (London, England) 365 (9474) (2005) 1877–1889.
[40] M.A. Konstam, J.E. Udelson, I.S. Anand, J.N. Cohn, Ventricular remodeling in heart failure: a credible surrogate endpoint, J. Card. Fail. 9 (5) (2003) 350–353.
[41] S.D. Anker, S. von Haehling, Inflammatory mediators in chronic heart failure: an overview, Heart (British Cardiac Society) 90 (4) (2004) 464–470.
[42] X. Fang, Z. Cai, H. Wang, D. Han, Q. Cheng, P. Zhang, F. Gao, Y. Yu, Z. Song, Q. Wu, P. An, S. Huang, J. Pan, H.Z. Chen, J. Chen, A. Linkermann, J. Min, F. Wang, Loss of cardiac ferritin H facilitates cardiomyopathy via Slc7a11-mediated ferroptosis, Circ. Res. 127 (4) (2020) 486–501.
[43] X. Fang, H. Ardehali, J. Min, F. Wang, The molecular and metabolic landscape of iron and ferroptosis in cardiovascular disease, Nat. Rev. Cardiol. 20 (1) (2023) 7–23.
[44] X. Fang, H. Wang, D. Han, E. Xie, X. Yang, J. Wei, S. Gu, F. Gao, N. Zhu, X. Yin, Q. Cheng, P. Zhang, W. Dai, J. Chen, F. Yang, H.T. Yang, A. Linkermann, W. Gu, J. Min, F. Wang, Ferroptosis as a target for protection against cardiomyopathy, Proc. Natl. Acad. Sci. U. S. A. 116 (7) (2019) 2672–2680.
[45] H. Zhang, P. Zhabyeyev, S. Wang, G.Y. Oudit, Role of iron metabolism in heart failure: from iron deficiency to iron overload, Biochimica et biophysica acta, Molecular Basis Disease 1865 (7) (2019) 1925–1937.
[46] X. Fang, P. An, H. Wang, X. Wang, X. Shen, X. Li, J. Min, S. Liu, F. Wang, Dietary intake of heme iron and risk of cardiovascular disease: a dose-response meta-analysis of prospective cohort studies, Nutrition, metabolism, and cardiovascular diseases, Nutr. Metabol. Cardiovasc. Dis. 25 (1) (2015) 24–35.
[47] L.R. Aldaba-Muruato, M.G. Moreno, M. Shibayama, V. Tsutsumi, P. Muriel, Allopurinol reverses liver damage induced by chronic carbon tetrachloride treatment by decreasing oxidative stress, TGF-β production and NF-κB nuclear translocation, Pharmacology 92 (3–4) (2013) 138–149.
[48] S.J. Dixon, B.R. Stockwell, The role of iron and reactive oxygen species in cell death, Nat. Chem. Biol. 10 (1) (2014) 9–17.
[49] C. Li, Z. Wu, H. Xue, Q. Gao, Y. Zhang, C. Wang, P. Zhao, Ferroptosis contributes to hypoxic-ischemic brain injury in neonatal rats: role of the SIRT1/Nrf2/GPx4 signaling pathway, CNS Neurosci. Ther. 28 (12) (2022) 2268–2280.
[50] W. Wang, X. Zhong, Z. Fang, J. Li, H. Li, X. Liu, X. Yuan, W. Huang, Z. Huang, Cardiac sirtuin1 deficiency exacerbates ferroptosis in doxorubicin-induced cardiac injury through the Nrf2/Keap1 pathway, Chem. Biol. Interact. 377 (2023) 110469.
[51] Y. Guo, M. Gupte, P. Umbarkar, A.P. Singh, J.Y. Sui, T. Force, H. Lal, Entanglement of GSK-3β, β-catenin and TGF-β1 signaling network to regulate myocardial fibrosis, J. Mol. Cell. Cardiol. 110 (2017) 109–120.

Abbreviations

Ang II: angiontensin II
ANOVA: one way analysis of variance
Bax: Bcl-2-associated X protein
Bcl-2: B cell lymphoma 2 protein
BW: body weight
CHF: chronic heart failure
CMs: primary cardiac myocytes
CO: cardiac output per minute
DHE: dihydroethidium
FBS: fetal bovine serum
Fe2+: reduced ferrous iron

Fer: ferritin
GAPDH: glyceraldehyde -3-phosphate dehydrogenase
GPX4: glutathione peroxidase 4
GSK-3β: glycogen synthase kinase-3β
H&E: haematoxylin and eosin
HF: heart failure
HW: heart weight
LVEF%: left ventricular ejection fraction
LVFS%: left ventricular fractional shortening
LVIDd: left ventricular internal dimension at diastole
LVIDs: left ventricular internal dimensions at systole
MDA: malondialdehyde
p-GSK-3β: phosphorylation of glycogen synthase kinase-3β
PLOOHs: hydrogen peroxide phospholipids
PTS: pterostilbene
ROS: reactive oxygen species
SEM: standard error
siRNA: small interference RNA
SIRT1: sirtuin 1
SIRTs: Sirtuins
TAC: transverse aortic constriction
TBST: tris-buffered saline-Tween
TEM: transmission electron microscope
TL: tibia length
WGA: wheat germ agglutinin
WT: wild-type